Synthesis and Photoisomerization Characteristics of a 2,4,4‘-Substituted Azobenzene Tethered to the Side Chains of Polymethacrylamide

ARTICLE *in* MACROMOLECULES · MAY 2006

Impact Factor: 5.8 · DOI: 10.1021/ma060169i

4 AUTHORS, INCLUDING:

Surjith Kumar
University of Alberta
10 PUBLICATIONS **262** CITATIONS
SEE PROFILE

Chang-Keun Lim
University at Buffalo, The State University of…
29 PUBLICATIONS **353** CITATIONS
SEE PROFILE

Synthesis and Photoisomerization Characteristics of a 2,4,4′-Substituted Azobenzene Tethered to the Side Chains of Polymethacrylamide

Surjith K. Kumar and Jong-Dal Hong*

Department of Chemistry, University of Incheon, 177 Dohwa-dong Nam-gu, Incheon 402-749, Korea

Chang-Keun Lim and Soo-Young Park

School of Materials Science and Engineering, Seoul National University, ENG 445, Seoul 151-744, Korea

Received January 23, 2006; Revised Manuscript Received March 13, 2006

ABSTRACT: A side-chain methacrylamide copolymer, poly{(*N*-[3-(4-(4′-methoxyphenylazo)-2-nitrophenoxy)-propyl]-*N*-[3-(dimethylamino)propyl]methacrylamide)-*co*-(*N*-[3-(dimethylamino)propyl]methacrylamide)} (PNA) functionalized with a 2,4,4′-substituted chromophore, 2-nitro-4′-methoxyazobenzene was prepared and characterized. The branched structure of the azo chromophore was specifically designed to prevent the aggregate formation by minimizing the ground-state aromatic stacking interactions between the azo molecules. This cationic polyelectrolyte, together with the oppositely charged *ι*-carrageenan (CAG) polysaccharide, was alternately dip-coated onto a fused silica substrate to produce a multilayered film by layer-by-layer electrostatic self-assembly. A UV/vis spectroscopic study of PNA, performed during both a heating−cooling (25−85 °C) and an *E*−*Z*−*E* photoisomerization cycle, revealed that the maximum absorbance wavelength of the chromophore did not shift in either DMSO/H_2O (1:20) solution or the multilayer assembly comprising 10 PNA/CAG bilayers. This result indicates that the PNA chromophores do not undergo aggregation. Monitoring of the *E*/*Z* photoisomerization of the solution- and film-based PNA chromophores revealed that the intensity of the $\pi-\pi^*$ transition band of its *E*-isomer decreased during irradiation with UV light. Also, the *Z*/*E* reverse isomerization induced by visible light ($\lambda > 460$ nm) was observed with almost full recovery of the *E* isomer. The kinetics of the photoisomerization step was determined to be monoexponential, indicating that photoisomerization proceeds via a single pathway. Unlike in general cases, one distinguishable property of the film-based PNA chromophore is the *E*/*Z* switching speed under experimental conditions (360 nm, $P = 2$ mW/cm^2), which is remarkably similar to that observed in solution.

1. Introduction

Stimulus-sensitive materials, especially those with light-affected properties, have been examined in numerous studies.[1−5] Azobenzene derivatives are a particularly interesting family of light-sensitive compounds, which have been widely investigated on account of their reversible *E*/*Z* photoisomerization and reorientation.[6] Since it was demonstrated in 1972 that the isomerization of various azobenzene chromophores bound to either the side chains or main chain of different polymers (poly(methyl methacrylate), poly(styrene), and certain polyesters) could be studied in solid state,[7] a large variety of spin-coated[8,9] and Langmuir−Blodgett (LB)-deposited[10−13] functionalized polymers have been studied. On the basis of the photoisomerization, polymeric thin films containing azobenzene chromophores have been found to exhibit diverse photoresponsive properties, which promise potential applications in areas such as holographic information storage,[14,15] photoswitching,[16,17] sensors,[18−20] wettability,[21,22] and liquid crystals alignment.[23−25]

About a decade ago, the layer-by-layer (LBL) electrostatic self-assembly (ESA) method was first proposed for the development of photosensitive azo materials due to the striking simplicity and versatility of this deposition method.[26,27] The first direction of LBL research was concerned with the kinetics of isomerization itself,[26−31] when an azo bolaamphiphile and polyionene were independently sandwiched between oppositely charged polyelectrolyte (PE) layers in LBL multilayer assemblies. A second investigation studied the reorientation of azobenzene chromophores in an attempt to establish whether these films exhibited promising optical storage properties,[26,32−34] or nonlinear optical effects.[35,36]

In general, azobenzene derivatives that contain an aromatic or dye chromophore, especially as a 4,4′-substituted type, tend to form relatively stable aggregates, when dispersed in aqueous media or incorporated into an organized assembly.[37−40] Extensive investigations have shown that these aggregates can be stabilized by strong noncovalent aromatic−aromatic interactions and tend to form readily in the presence of water.[41] This aggregation process can be described semiquantitatively by the exciton model introduced by Kasha.[42] The free volume around the chromophore appears to be essential for photoisomerization in organized solid films.[43,44] As an example, the *E*/*Z* photoisomerization of synthetic azobenzene-derivatized phospholipids is much slower (30−130-fold) when the phospholipids are incorporated into the bilayers rather than being free in solution (e.g., in chloroform).[43] Thus, various molecular engineering approaches have been employed to mimic this free volume. These include self-assembly,[45] the guest−host approach,[46] the mixed LB film approach,[47] and the use of spacer groups on the photosensitive materials.[48] In a previous publication,[33] it was also reported that the aggregation of azo chromphores strongly influences the kinetics of *E*/*Z* photoisomerization and the reorientation of azobenzene moieties in the LBL-deposited multilayers of membrane-forming polyionenes (−[$(CH_2)_n$−O−Az═Az−O−$(CH_2)_n$−NR_2]−) when the spacer length (*n*) was extended from 6 to 10 and 12 carbons. An additional influence of electrostatic and H-bonding interactions on the optical storage

10.1021/ma060169i CCC: $33.50
Published on Web 04/01/2006

Scheme 1. Synthesis Route of [4-(3-Bromopropoxy)-2-nitrophenyl]-(4′-methoxyphenyl)diazene (6)

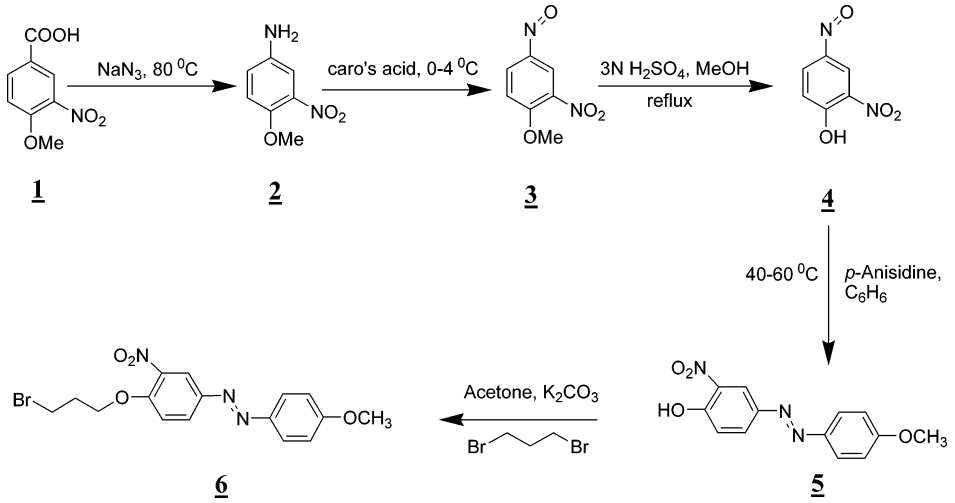

capability of an azo polymer was also observed in LBL-deposited multilayer of PEs.[32]

Here, we describe the synthesis of a purposely designed donor−acceptor type chromophore, 2-nitro-4′-methoxyazobenzene. Moreover, the branched structure of this strongly dipolar chromophore is designed to prevent the azo chromophores from forming aggregates by minimizing the ground-state aromatic stacking interactions between them through steric effects. The chromophore was linked to the side chain of a methacrylamide to give the cationic layer component of LBL assembly; poly-{(*N*-[3-(4-(4′-methoxyphenylazo)-2-nitrophenoxy)propyl]-*N*-[3-(dimethylamino)propyl]methacrylamide)-*co*-(*N*-[3-(dimethylamino)propyl]methacrylamide)}, PNA (Scheme 1). Here, we will mainly describe the synthesis of PNA and also the *E/Z* photoisomerization properties of this chromophore both in solution and in LBL-deposited multilayer films. The photoreorientation property of PNA in the multilayer assemblies will be described in a forthcoming publication.

2. Experimental Section

2.1. Materials. All materials are purchased from Aldrich. Tetrahydrofuran (THF) was distilled over sodium benzophenone ketyle. Dimethyl sulfoxide was purified by distillation under reduced pressure. Poly(allylamine hydrochloride), PAH (M_n = 50 000−65 000), and ι-carrageenan, CAG, were used without further purification.

2.2. Synthesis. Scheme 1 represents synthetic route for the chromophore **6** based on modification of methods described by Sternhell et al.[49,50] The versatility of this synthetic method was demonstrated by the preparation of compounds **2**−**4**, which is in detail described in supplementary data I (Supporting Information), together with a detailed structural analysis. The chromophore **6** was prepared by the Williamson's ether synthesis of **5** with 1,3-dibromopropane in anhydrous acetone, in the presence of K_2CO_3 and KI.

(1) 4-(4′-Methoxyphenylazo)-2-nitrophenol (5). 2-Nitro-4-nitrosophenol, **4** (500 mg, 3.0 mmol), *p*-anisidine (500 mg, 4.1 mmol), and acetic acid (4 drops) were placed together in a reaction flask and dissolved in benzene (20 mL). The reaction mixture was poured into water after warming at 40−50 °C for 1 h and extracted with ether until the extracts were colorless. The extracts were then dried over $MgSO_4$ and evaporated to give a dark brown solid. The column chromatography (EA:Hex = 1:4) gave ***5*** as red crystals (480 mg, 59% yield). ^{1}H NMR ($CDCl_3$): δ (ppm) = 10.80 (s, 1H, Ar−O**H**), 8.66 (s, 1H, Ar−**H** of azobenzene), 8.16 (d, 1H, Ar−H of azobenzene), 7.92 (d, 2H, Ar−H of azobenzene), 7.27 (d, 1H, Ar−H of azobenzene), 7.02 (d, 2H, Ar−H of azobenzene), 3.91 (s, 3H, Ar−O-Me). ^{13}C NMR ($CDCl_3$): δ (ppm) = 162.76, 156.45, 146.75, 145.92, 133.86, 130.81, 125.21, 120.72, 120.52, 114.58, 55.86. FTIR: υ (cm^{-1}) = 3343 (−OH str), 3059 (aromatic str), 1579 (benzene C=C str), 1535, 1348 (−NO_2 str), 1260 (C−O− str).

(2) 4-[1-(3-Bromopropoxy)-2-nitrophenyl](4′-methoxyphenyl)-diazene (6). A solution of **5** (200 mg, 0.7 mmol) and K_2CO_3 (304 mg, 2.2 mmol) in 20 mL of dry acetone was placed in a 100 mL three-necked round-bottomed vessel under dry nitrogen and refluxed for 1 h. Then, 1,3-dibromopropane (207 mg, 1.0 mmol) diluted in 2 mL of dry acetone was added dropwise, and the resulting solution was refluxed for 4 days. The reaction mixture was diluted with water (30 mL) and extracted with ether. The organic layer was washed first with water and then brine and finally dried over $MgSO_4$. The organic solvent was removed under reduced pressure, and the solid crude product was purified by column chromatography on silica gel with using ethyl acetate/petroleum ether (1:5) mixture as the eluent to give **6** in 51% yield (with respect to **5**) as orange crystals (mp 137 °C). ^{1}H NMR ($CDCl_3$): δ (ppm) = 8.39 (s, 1H, Ar−**H** of azobenzene), 8.10 (d, 1H, Ar−**H** of azobenzene), 7.90 (d, 2H, Ar−**H** of azobenzene), 7.20 (d, 1H, Ar−**H** of azobenzene), 7.01 (d, 2H, Ar−**H** of azobenzene), 4.34 (t, 2H, Ar−O−**CH_2**), 3.91 (s, 3H, Ar−O−**Me**), 3.68 (t, 2H, −**CH_2**−Br), 2.39 (m, 2H, −O−CH_2−**CH_2**−CH_2−Br). ^{13}C NMR ($CDCl_3$): δ (ppm) = 162.465, 153.064, 145.554, 145.056, 140.821, 128.875, 124.936, 119.042, 114.360, 114.315, 67.138, 55.601, 31873, 29.628. FTIR: υ (cm^{-1}) = 3059 (aromatic str), 2970, 2898 (C−H str), 1529 (aromatic asym str), 1510 (−NO_2 str), 1280 (−Ph−O−C− str). EA: Found: C, 48.39; H, 4.19; N, 9.9%. Calcd for $C_{16}H_{16}BrN_3O_4$: C, 48.75; H, 4.09; N, 10.66%.

(3) Poly(*N*-[3-(dimethylamino)propyl]methacrylamide), 7. The homopolymerization of the purified commercially available monomer *N*-[3-(dimethylamino)propyl]methacrylamide was carried out using 2,2′-azobis(isobutyronitrile) (AIBN) free radical initiator in dry THF, in accordance with the literature methods.[51] A detailed description of the synthesis and the characterization of the compound **7** is given in supplementary data II (Supporting Information). The number-average molecular weight of **7** was determined by gel permeation chromatography to be 6.35 × 10^4 with a polydispersity index of 1.2.

(4) Poly{(*N*-[3-(4-(4′-Methoxy-phenylazo)-2-nitrophenoxy)-propyl]-*N*-[3-(dimethylamino)propyl]methacrylamide)-*co*-(*N*-[3-(dimethylamino)propyl]methacrylamide)}, PNA (8). PNA was prepared by a quaternization reaction of **7** with **6** in dry ethanol, as shown in Scheme 2. A reaction mixture of **7** (250 mg, 1.5 mmol) and **6** (579 mg, 1.5 mol) in 10 mL of dry ethanol was stirred at 45 °C for 7 days. A yellow precipitate was filtered off, redissolved in DMSO, and precipitated in ethanol or THF. The purification procedure was repeated for several times until no further trace of **6** was found. The purified polymer was dried under high vacuum to give a yellow powder (521 mg, 35% yield). The polymer was

Scheme 2. Synthesis Route of Poly{(*N*-[3-(4-(4′-methoxyphenylazo)-2-nitrophenoxy)propyl]-*N*-[3-(dimethylamino)propyl]methacrylamide)-*co*-(*N*-[3-(dimethylamino)propyl]methacrylamide)}, PNA (8)

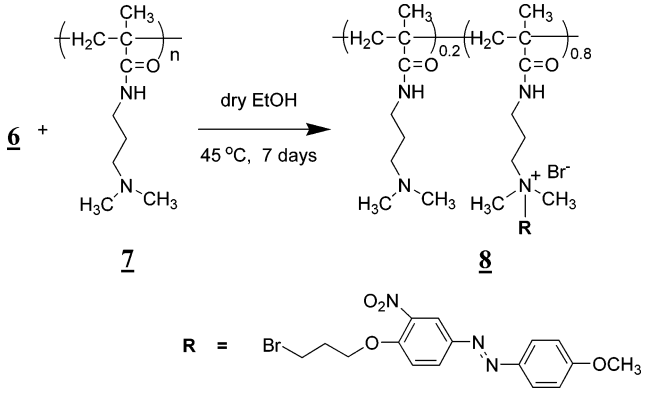

characterized by ^{1}H NMR at 65 °C and FT-IR spectroscopy. ^{1}H NMR (DMSO-d_6): δ (ppm) = 8.1 (s, 1H, Ar−**H** for azobenzene), 7.99 (d, 1H, Ar−**H** for azobenzene), 7.72 (d, 2H, Ar−**H** for azobenzene), 7.51 (d, 1H, Ar−**H** for azobenzene), 7.01 (d, 2H for azobenzene), 4.34 (t, 2H Ar−O−**CH$_2$**−), 3.79 (s, 3H, Ar−O−**Me**), 3.5−3.7 (br, −CON−**CH$_2$**−, −N−**CH$_2$**−, −N$^+$−**CH$_2$**−), 3.2 (s, **CH$_3$**−N$^+$−**CH$_3$**), 2.21 (s, **CH$_3$**−N−**CH$_3$**), 2.18−1.19 (br, −CH$_3$ backbone), 1.3−0.8 (br, −**CH$_2$**− backbone, −CON−CH$_2$−**CH$_2$**−CH$_2$−, −O−CH$_2$−**CH$_2$**− CH$_2$−). FTIR: υ (cm^{-1}) = 3059 (aromatic str), 2980−2891 (br, C−H str), 2851 (s, −CH$_3$), 1690 (C═O amide str), 1530 (−N$^+$−CH$_3$), 1260 (Ph−O−C).

2.3. Electrostatic Self-Assembled Multilayer. The ultrapure water used for all experiments and cleaning steps was obtained using an ion exchange and filtration unit (Milli-Q, Millipore GmbH) to give a resistivity better than 18.0 MΩ·cm. The substrates selected for all adsorption experiments were fused silica slides of size 25 × 50 mm^2. The substrates were cleaned by ultrasonication in a mixture of H_2SO_4/H_2O_2 (7/3) and then heated in the mixture of $H_2O/H_2O_2/NH_3$ (5:1:1) at 80 °C for 1 h. The substrates were thoroughly washed with ultrapure water after both steps.

A typical assembly started with a cleaned fused silica slide with five bilayers of PAH/CAG that were spin-assembled alternately from aqueous solution of PAH (1 unit mM, pH 4.0) and CAG (1 unit mM, pH 6.3) for 15 s. Then, the slide was dipped into a 1 mM PNA DMSO/H_2O (1:20) solution for 20 min. After that, the nonspecifically adsorbed material was washed away by dipping the slide first into a (1:20) DMSO/H_2O mixture three times and then finally into water for 1 min. An anionic PE layer was then deposited by dipping the slide into a 5 mM CAG solution in order to promote the subsequent multilayer deposition. After each adsorption step, the surface of the film was thoroughly dried with a gentle stream of nitrogen gas. The quantity of material deposited at each step was deduced from its absorption spectrum, which was determined using a Perkin-Elmer UV/vis spectrophotometer (Lambda 40).

2.4. Methods. Thermal analysis of the polymer was performed using differential scanning calorimetry (TA Instruments, SC-2910) at a heating rate 10 °C/min in a nitrogen atmosphere and calibrated using an indium standard. The molecular weight of the polymer was measured using gel permeation chromatography (Waters, M515); THF was used as the eluting solvent at a rate of 1.0 mL/min. Calibration was performed using polystyrene standard. UV/vis spectra were recorded on a Perking-Elmer spectrometer (Lambda 40).

The thickness of the multilayer films on silicon wafers was measured by using a spectroscopic ellipsometer (Nano-View, SMG-1000), equipped with a 350−820 nm irradiation source set at an incident angle of 60°. Employing a homemade computer program, the elliptical azimuth Ψ and phase angle were determined for both the bare clean substrate and the multilayer films, and these experimental values were used to calculate the corresponding film thicknesses. At least 3−5 different sampling points were considered in order to obtain an average thickness value.

Photoisomerization of the polymer both in solution and in the multilayer film was carried out using a high-pressure Hg−Xe lamp (Oriel, 500 W), equipped with a UV35 band-pass filter and a sharp cut Y46 glass filter (Shimadzu Co.) for UV and visible light irradiation, respectively. The power densities of the incident light were adjusted to 2 mW/cm^2 for UV and 100 mW/cm^2 for visible light using an optical power meter (Melles Griot, 13PEM001).

3. Results and Discussion

3.1. Synthesis and Characterization of PNA. The synthetic route of the azo polyelectrolyte PNA is given in Schemes 1 and 2. The nitroazobenzene chromophore **6** was isolated as orange crystals and demonstrated good solubility in most organic solvents. PNA was obtained from the polymer-analogous reaction between **6** and polymethacrylamide **7**. The molecular structure and composition of PNA were identified using ^{1}H and ^{13}C NMR spectroscopy. A notable chemical downfield shift (from 2.25 to 3.17 ppm) was observed for the quaternized *N*,*N*-dimethyl protons tethered to the amino group of **7**, as revealed in Figure 1. The degree of the quaternization was estimated to be about 80% on the basis of the integral of the signal for the methyl group tethered to the amine, before and after the quaternization. One possible reason for the lack of complete quaternization is steric hindrance between the polymeric chains and the bulky azo reactant.

PNA shows good solubility in DMSO and DMF, but not in water. Differential scanning calorimetry (DSC) analysis of PNA revealed it was thermally stable up to 221 °C (under nitrogen, heating rate = 10 °C/min) but underwent degradation at higher temperatures. There is also no clear endothermic peaks on DSC, which was also found in a cationic azobenzene-derivatized polyelectrolyte.[52]

3.2. Electrostatic Self-Assembled Multilayer. The layer-by-layer deposition of PNA/CAG bilayers is examined on the basis of their UV/vis spectra (Figure 2a), where PEs have been deposited on a fused silica substrate using a solution-dip electrostatic self-assembly method.[53,54] A plot of maximum absorbance of the PNA layer at 355 nm vs number of deposition cycles revealed the deposition to be uniform. Again, a linear increase in absorbance demonstrates that the deposition process proceeded regularly, as shown in Figure 2b. The thickness of the deposited bilayers increased uniformly with the number of the adsorption cycles, as determined by optical ellipsometry (Figure 2c). The average thickness of a PNA/CAG bilayer was determined to be 1.91 nm, which is in good agreement with the typical value for polelectrolyte bilayers.

3.3. Thermal Stability. The thermal stability of PNA in both solution and multilayer films was investigated by performing a heating−cooling cycle in the range 25−85 °C on the samples. The samples were allowed to equilibrate for 1 h after each temperature has been reached. Small changes in the intensity

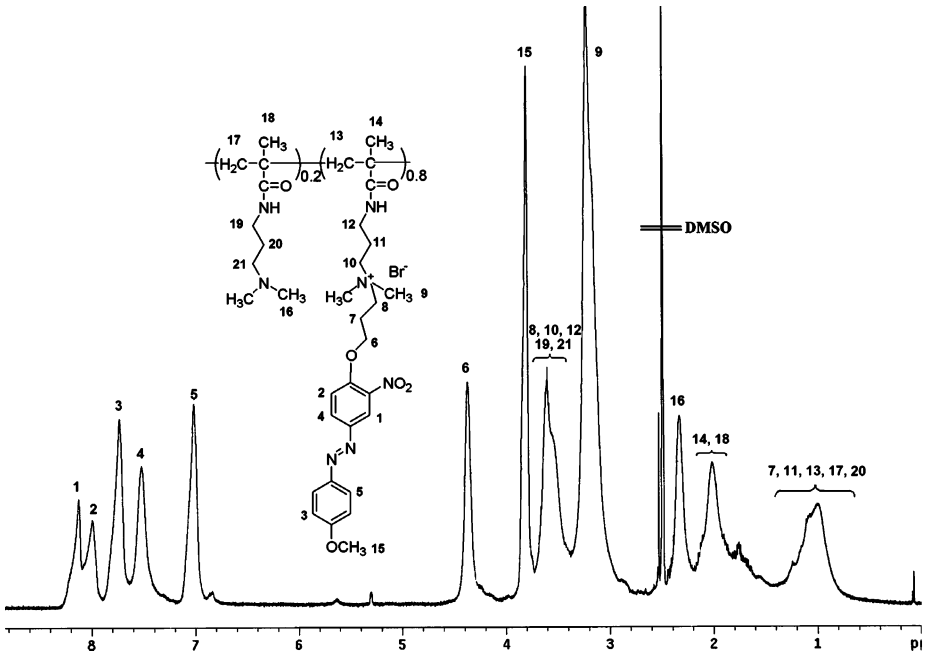

Figure 1. ^{1}H NMR spectrum of PNA in DMSO-d_6 at 65 °C.

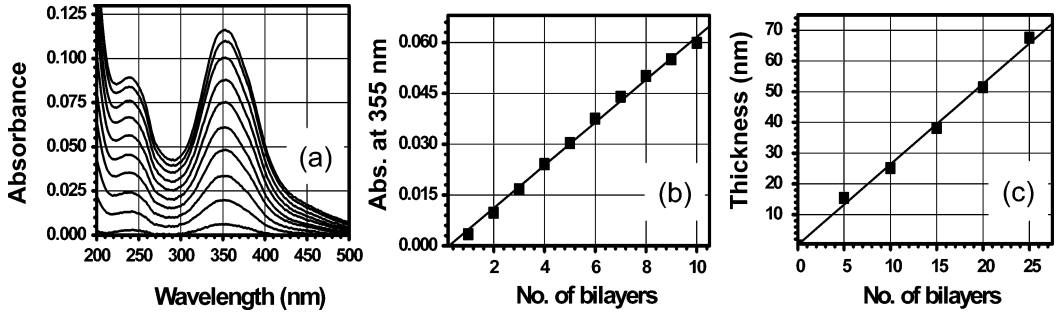

Figure 2. (a) UV/vis spectra of a PNA/CAG multilayered systems prepared by varying the number of the deposition cycles. (b) The relationship between the maximum absorbance of the multilayer assemblies at 355 nm and the number of PNA/CAG bilayers. (c) Ellipsometric thickness vs the number of PNA/CAG bilayers deposited on a silicon substrate.

of the maximum absorbances at 344 nm (solution) and at 355 nm (film) appeared with increasing temperature, as shown in the plot of maximum absorbance vs temperature (Figure 3). The increase of the maximum absorbance would be most probably due to conversion of a small *Z* population to *E* during the heating process. The original conformation of the chromophore was almost recovered on cooling. This suggests that the chromophore exhibits a possible preferential conformation in both the solution and the multilayer assembly, which could be transformed to a second one at a higher temperature. Here, it should also be noted that, in the case of the multilayer film, an additional conformational transition temperature was observed near 50 °C during the heating and cooling process.

In the heating steps on both samples, no shift of wavelength at maximum absorbance was observed, indicating a lack of aggregate formation. The (H- or J-type) aggregate state of azobenzene derivatives has in general been predicted from the effects of temperature and/or isomerization cycling on the wavelength shift at the maximum absorbance. This takes into account the fact that the aggregates of azobenzene chromophores in solution or in thin film could be thermally or photochemically destroyed to form a molecularly dispersed state.[33,55]

3.4. Photoisomerization Characteristics of PNA in Solution and in Multilayer Assemblies. The *E/Z* photoisomerization of PNA in a DMSO/H_2O (1/20) solution (0.001 mM) and in a multilayer assembly composed of 10 PNA/CAG bilayers is investigated, while irradiating the sample with UV light (360 nm, $P = 2$ mW/cm^2). Absorption spectra of PNA in the solution (Figure 4a) are characterized by a very weak n$-\pi^*$ transition band at 460 nm, the $\pi-\pi^*$ band at 344 nm, and a $\Phi-\Phi^*$ band at 251 nm. However, a bathochromic shift of the $\pi-\pi^*$ transition band from 344 to 355 nm is observed in Figure 4b for the multilayer film. This is most probably due to solvatochromism, since no aggregate formation of the chromophores was evident during the temperature study or the *E/Z* photoisomerization cycle effect on the wavelength at the maximum absorbance.

The two n$-\pi^*$ and $\pi-\pi^*$ transitions in the UV/vis spectra of PNA/CAG multilayer film (Figure 4b) are directed approximately along the long molecular axis of *E*-azobenzene chromophore. In contrast, the $\Phi-\Phi^*$ absorbance at 235 nm corresponds to the electronic transition moment roughly parallel to the short axis of the *E*-azobenzene chromophore.[56] This makes it reasonable to expect that, in contrast to the $\pi-\pi^*$ transition, the $\Phi-\Phi^*$ transition of the aromatic cores will be independent of the chromophores orientation. The ratio of $\pi-\pi^*/\Phi-\Phi^*$ for PNA in the (1:20) DMSO/H_2O solution (1.65) is slightly greater than that observed in the multilayer assembly (1.27), where the rodlike chromophores exhibit a strong preference for an out-of-plane orientation.

During *E/Z* photoisomerization, a spectral change occurs with a progressive decrease in the $\pi-\pi^*$ transition band. However,

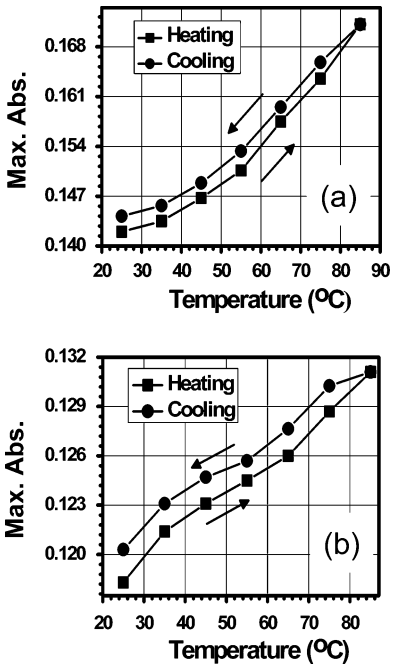

Figure 3. Maximum absorbances of the $\pi-\pi^*$ transition peak during a heating−cooling cycle, as a function of the investigated temperature: (a) PNA in 1:20 DMSO/H_2O (0.001 mM); (b) 10 PNA/CAG bilayers film in H_2O.

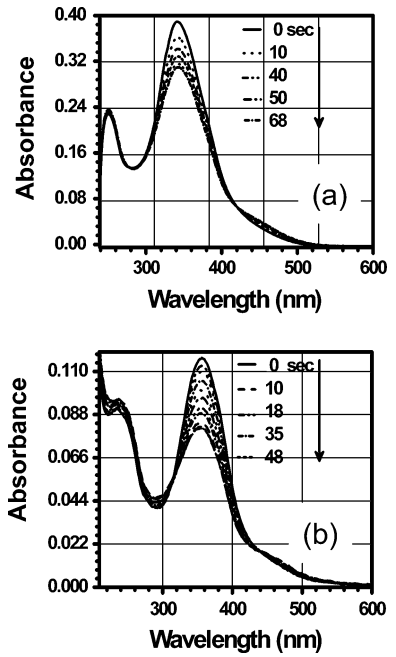

Figure 4. UV−vis spectra of 0.001 mM PNA DMSO/H_2O (1:20) (a) and a 10 PNA/CAG multilayer film (b) recorded over different time intervals irradiated with 360 nm UV light (P = 2 mW/cm^2).

the band does not completely disappear even after prolonged irradiation, indicating that the photoreaction is incomplete. The calculation according to ref 57 shows that 30% of *E* isomers in the virgin film are transformed to *Z*-isomeric form, which is slightly different from the 36% transformation observed in solution. The incomplete $E-Z$ photoisomerization cannot be fully elucidated at this moment due to the lack of directly comparable 2-substituted azobenzene systems in the literature. However, it could be understood at a certain level on the basis of mechanistic studies of the $E-Z$ isomerization of azobenzene with different electron-withdrawing substituents attached to the para-positions of the chromophores by Ho et al.[58] The phenomenon of incomplete $E-Z$ photoisomerization was found to exist only in the nitro-substituted azobenzene systems, in accordance with the abundant other examples in the literature.[29,58,59] A strong electron-withdrawing substituent would reduce the double-bond character of the azo group and provide a favorable condition for the transition state involved the rotation mechanism that is joined by a N−N single bond. The intermediate in the transition state can flip to either *E* or *Z* isomer by free rotation, with roughly the same activation energy. It was clearly demonstrated that only through a rotation mechanism could a mixture of *E/Z* isomers be obtained from the photochemical isomerization of *E* isomers, whereas a *Z* isomer would be the sole product if the isomerization proceeded via an inversion pathway.[58]

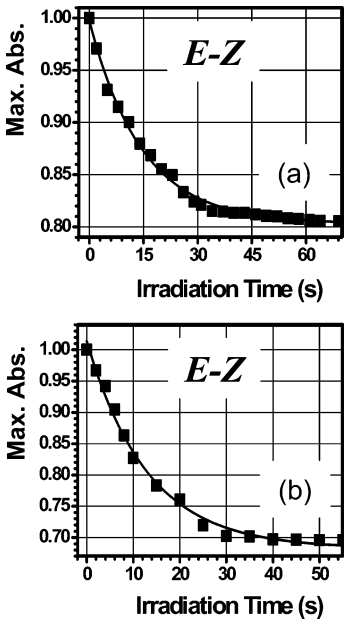

Figure 5. Normalized maximum absorbance of 0.001 mM PNA DMSO/H_2O (1:20) (a) and a 10 PNA/CAG bilayer film (b) recorded over different time intervals. The solid lines represent the fitted curves.

The rates of photoisomerization depend on the local environments of the chromophores and the chromophore phase itself. The $E-Z$ photoisomerization kinetics of PNA in the (1:20) DMSO/H_2O mixture was compared with that in a 10 PNA/CAG bilayer film, as shown in Figure 5. By comparing the maximum intensities of the $\pi-\pi^*$ transition band of PNA in solution and in multilayer films, it was observed that both intensities decrease on exposure to UV irradiation and that the amount of decrease was dependent on the irradiation time interval (denoted here as A_1). It is known that the photoinduced isomerization of azobenzene usually follows first-order kinetics in solution.[60] The best fit of the experimental points for PNA in solution as well as in film was obtained by simulating the absorbance (A) data with the following first-order exponential decay function:

$$A(t) = A_0 + A_1 \exp(-t/T_1) \quad (1)$$

The results obtained from the best fit are listed in Table 1. A wavelength-dependent photostationary state between both *E/Z* isomers is established for both cases after about 50 s irradiation. PNA is a highly photosensitive nitroazobenzene chromophore with relatively fast photoresponsiveness in comparison with copolymers[29,58,59] containing the para-substituted nitroazobenzene which show no significant photochromic effect. The flexible photochromism of the nitro-containing azo chromophore is possibly attributed to the branched structure of the 2-nitro-

Table 1. Parameters of Photoisomerization Kinetics Obtained from the Curve Fitting

photoisomerization	sample	A_0	A_1	T_1 (s)	χ^2
$E-Z$	solution	$(0.311 \pm 0.5) \times 10^{-3}$	$0.075 \pm 1 \times 10^{-3}$	14.6 ± 0.4	2.1×10^{-6}
	multilayer	$(0.079 \pm 0.8) \times 10^{-3}$	$0.039 \pm 1 \times 10^{-3}$	13.3 ± 0.1	1.4×10^{-6}
$Z-E$	solution	$(0.388 \pm 0.5) \times 10^{-3}$	$-0.078 \pm 1 \times 10^{-3}$	8.9 ± 0.2	1.4×10^{-6}
	multilayer	$(0.118 \pm 0.9) \times 10^{-3}$	$-0.037 \pm 1 \times 10^{-3}$	5.7 ± 0.5	1.9×10^{-6}

Table 2. Parameters of the Thermal *Z*−*E* Back-Isomerization Kinetics Obtained from the Curve Fitting

thermal isomerization	sample	A_0	A_1	T_1 (h)	χ^2
$Z-E$	solution	$(0.437 \pm 7) \times 10^{-3}$	$(-0.138 \pm 6) \times 10^{-3}$	22.1 ± 1.9	1.7×10^{-6}
	multilayer	$(0.118 \pm 2) \times 10^{-4}$	$(-0.037 \pm 3) \times 10^{-4}$	13.2 ± 3.3	2.9×10^{-7}

azobenzene, which minimizes the $\pi-\pi^*$ interaction between chromophores and creates a free space within the matrix. Here, it is worth noting that the time constant (14.6) for T_1 in solution is comparable with that (13.3) obtained in the multilayer film, which is expected since the photoisomerization has generally been observed to occur much more slowly in films than in solutions.[29] The subsequent irradiation of the chromophore in both solution- and film-based PNA with visible light ($\lambda = 470$ nm, $P = 100$ mW/cm^2) showed an almost complete recovery to the virgin state due to the *Z/E* back-isomerization. It was also found that no significant spectral change was observed in both cases after the five $E-Z-E$ photoisomerization cycles, as shown in supplementary data III (Supporting Information). The experimental data points are also fitted to the first-order exponential decay function (1). The results obtained from the best fit are collected in Table 1.

The thermal *Z*-to-*E* reverse isomerization was studied in the dark by monitoring the recovery of the $\pi-\pi^*$ absorption band of PNA at 344 nm (in solution) and 355 nm (in film), after the photostationary state had been obtained under UV light irradiation. The *Z*-isomers tend to rebuild the thermodynamically stable isomeric conformation during storage in the dark. Both samples showed almost complete recovery in the maximum absorbance: 98% for solution and 97% for film, as revealed in Figure 6. The back-isomerization was also fitted to the first-order exponential decay function (1) (Figure 6). The reults obtained from the best fit are summarized in Table 2. It was found that the thermal *Z/E* isomerization of PNA proceeds much faster in multilayer film than in solution, indicating a dependence on the local environment of the chromophores. The thermal *Z/E* isomerization in the films can be attributed to the trapping of some portion of *Z* isomers in a constrained environment within the film.[7,61,62]

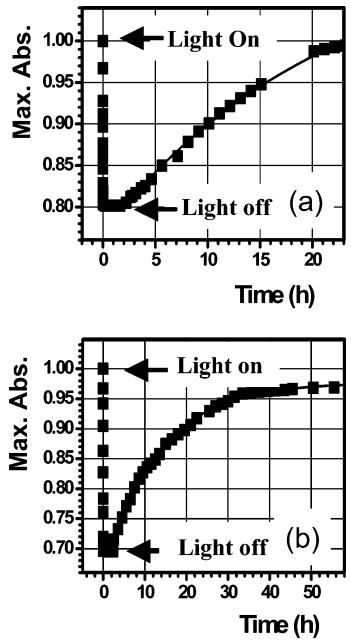

Figure 6. Maximum absorbance of a 0.001 mM PNA solution (1:20 DMSO/H_2O) at 344 nm (a) and of a multilayer film composed of alternate PNA/CAG at 355 nm (b) over different time intervals in the dark at room temperature. The solid lines in the relaxed part of the plot represent the fitted curves.

4. Summary and Conclusions

A side-chain methacrylamide copolymer, poly{(*N*-[3-(4-(4′-methoxyphenylazo)-2-nitrophenoxy)propyl]-*N*-[3-(dimethylamino)propyl]methacrylamide)-*co*-(*N*-[3-(dimethylamino)propyl]-methacrylamide)} (PNA), functionalized with a 2,4,4′-substituted chromophore, 2-nitro-4′-methoxyazobenzene, has been successfully prepared and characterized. This cationic polyelectrolyte (PNA) was alternately dip-coated along with the oppositely charged polyelectrolyte CAG on a fused silica substrate to obtain a multilayered film via layer-by-layer deposition, where each step of the procedure was monitored by UV/vis spectroscopy. The thickness of a PNA/CAG bilayer was determined to be 1.91 nm using ellipsometry, assuming the refractive index of the polyelectrolytes to be 1.52.

The *E/Z* isomerization of PNA in both solution and film was induced by UV irradiation (360 nm, $P = 1$ mW/cm^2). The subsequent irradiation with visible light (460 nm, 100 mW/cm^2) and the ensuing thermal relaxation resulted in *Z/E* reverse isomerization. A study of the temperature and photochemical effects on UV/vis absorbance spectra of PNA revealed that the chromophore does not form aggregates in either solution or multilayer assemblies due to the steric hindrance of the nitro group in the 2-position on the azobenzene. It was also found that the chromophores are in a molecularly dispersed state with no preferential orientation, as determined from the polarized UV/vis spectroscopy. The high photochromism and good photoresponsiveness of the nitro-containing azobenzene chromophores are ascribed to the alkoxy group located in the 4′-position, which is known to enhance both properties.[29]

The kinetics of *E*/*Z* and *Z*/*E* photoisomerization are first order in solution as well as in the multilayer film. It is worth mentioning that the *E*/*Z* switching speed of PNA in the film was comparable to that observed in solution, indicating that the photoisomerization process occurs via an equivalent mechanism.

Acknowledgment. This work was supported by a grant (no. R05-2003-000-10848-0) from the Korea Science and Engineering Foundation. We are very grateful to Prof. Il-Sin Ahn and co-workers at Hanyang University for allowing us to use his ellipsometer.

Supporting Information Available: Preparation of compounds **2**−**4** and **7** and figure of fully reversible *E*/*Z* and *Z*/*E* photoisomerization cycles. This material is available free of charge via the Internet at http://pubs.acs.org.

References and Notes

(1) Xie, S.; Natansohn, A.; Rochon, P. *Chem. Mater.* **1993**, *5*, 403.
(2) Kumar, G. S.; Neckers, D. C. *Chem. Rev.* **1989**, *89*, 1915.
(3) Anzai, J.; Osa, T. *Tetrahedron* **1994**, *50*, 4039.
(4) Sata, T. *J. Membr. Sci.* **2000**, *167*, 1.
(5) Natansohn, A.; Rochon, P. *Can. J. Chem.* **2001**, *79*, 1093.
(6) Natansohn, A.; Rochon, P. *Chem. Rev.* **2002**, *102*, 4139.
(7) Paik, C. S.; Morawetz, H. *Macromolecules* **1972**, *5*, 171.
(8) Kimura, K.; Suzuki, T.; Yokoyama, M. *J. Phys. Chem.* **1990**, *94*, 6090.
(9) Menzel, H.; Hallensleben, M. L.; Schmidt, A.; Knoll, W.; Fischer, T.; Stumpe, J. *Macromolecules* **1993**, *26*, 3644.
(10) Ichimura, K.; Momose, M.; Kudo, K.; Akiyama, H.; Ishizuki, N. *Thin Solid Films* **1996**, *284*, 557.
(11) Shimomura, M.; Kunitake, T. *Thin Solid Films* **1985**, *132*, 243.
(12) Sawodny, M.; Schmidt, A.; Urban, C.; Ringsdorf, H.; Knoll, W. *Makromol. Chem., Macromol. Symp.* **1991**, *46*, 217.
(13) Takahiro, S.; Masako, S.; Yuji, K.; Takashi, T.; Ryoichi, F.; Ichimura, K.; Suzuki, Y. *Langmuir* **1993**, *9*, 211.
(14) Wang, C.; Fei, H.; Yang, Y.; Wei, Z.; Qiu, Y.; Chen, Y. *Opt. Commun.* **1999**, *159*, 58.
(15) Nikolova, L.; Nedelchev, L.; Todorov, T.; Petrova, T.; Tomova, N.; Dragostinova, V.; Ramanujam, P. S.; Hvilsted, S. *Appl. Phys. Lett.* **2000**, *77*, 657.
(16) Sagues, F.; Albalat, R.; Reigada, R.; Crusats, J.; Mullol, J. I.; Claret, J. *J. Am. Chem. Soc.* **2005**, *127*, 5296.
(17) Shimoboji, T.; Ding, Z. L.; Stayton, P. S.; Hoffman, A. S. *Bioconjugate Chem.* **2002**, *13*, 915.
(18) Gunnlaugsson, T.; Leonard, J. P.; Murray, N. S. *Org. Lett.* **2004**, *6*, 1557.
(19) Mermut, O.; Barrett, C. J. *Analyst* **2001**, *11*, 1861.
(20) Bradford, A.; Drake, P. L.; Worsfold, O.; Peterson, I. R.; Walton, D. J.; Price, G. *J. Phys. Chem. Chem. Phys.* **2001**, *9*, 1750.
(21) Feng, C. L.; Zhang, Y. J.; Jin, J.; Song, Y. L.; Xie, L. Y.; Qu, G. R.; Jiang, L.; Zhu, D. B. *Langmuir* **2001**, *17*, 4593.
(22) Ichimura, K.; Oh, S. K.; Nakagawa, M. *Science* **2000**, *288*, 1624. (b) Oh, S. K.; Nakagawa, M.; Ichimura, K. *J. Mater. Chem.* **2002**, *12*, 2262.
(23) Han, M.; Ichimura, K. *Macromolecules* **2001**, *34*, 82.
(24) Eich, M.; Wendroff, J. H.; Beck, B.; Ringsdorf, H. *Makromol. Chem. Rapid Commun.* **1987**, *8*, 59.
(25) Todorov, T.; Nikolova, L.; Tomova, N. *Appl. Opt.* **1984**, *23*, 4309.
(26) Hong, J. D.; Park, E. S.; Park. A. L. *Bull. Korean Chem. Soc.* **1998**, *19*, 1156.
(27) Hong, J. D.; Jung, B. D.; Kim, C. H.; Kim, K. *Macromolecules* **2000**, *33*, 7905.
(28) Dante, S.; Advincula, R.; Frank, C. W.; Stroeve, P. *Langmuir* **1999**, *15*, 193.
(29) Wu, L.; Tuo, X.; Cheng, H.; Chen, Z.; Wang, X. *Macromolecules* **2001**, *34*, 8005.
(30) Suzuki, I.; Ishizaki, T.; Hoshi, T.; Anzai, J. *Macromolecules* **2002**, *35*, 577.
(31) Jung, B. D.; Hong, J. D.; Voigt, A.; Leporatti, S.; Dahne, L.; Donath, E.; Mohwald, H. *Colloids Surf., A* **2002**, *198*−*200*, 483.
(32) Zucolottoa, V.; Mendonc, C. R.; Santos, D. S., Jr.; Balogh, D. T.; Zilio, S. C. Oliveira, Jr. O. N.; Constantino, C. J. L.; Aroca, R. F. *Polymer* **2002**, *43*, 4645.
(33) Jung, B. D.; Stumpe, J.; Hong, J. D. *Thin Solid Films* **2003**, *441*, 261.
(34) Wang, H.; He, Y.; Tuo, X.; Wang, X. *Macromolecules* **2004**, *37*, 135.
(35) Balasubramanian, S.; Wang, X.; Wang, H. C.; Yang, K.; Kumar, J.; Tripathy, S. K. *Chem. Mater.* **1998**, *10*, 1554.
(36) Lee, S. H.; Balasubramanian, S.; Kim, D. Y.; Viswanathan, N. K.; Bian, S.; Kumar, J.; Tripathy, S. K. *Macromolecules* **2000**, *33*, 6534.
(37) Heesemann, J. *J. Am. Chem. Soc.* **1980**, *102*, 2167.
(38) Fukuda, K.; Nakahara, H. J. *Colloid Interface Sci.* **1980**, *98*, 555.
(39) Kunitake, T. *Angew. Chem., Int. Ed. Engl.* **1992**, *31*, 709.
(40) Song, X.; Perlstein, J.; Whitten, D. G. *J. Am. Chem. Soc.* **1995**, *117*, 7816.
(41) Chen, H.; Liang, K.; Song, X.; Smha, H.; Law, K. Y.; Perlstein, J.; Whitten, D. G. In *Micelles, Microemulsions and Monolayers: Science and Technology*; Shah, D., Ed.; Marcel Dekker: New York, 1995.
(42) MacRae, E. G.; Kasha, M. In *Physical Processes in Radiation Biology*; Academic: New York, 1964; p 23.
(43) Song, X.; Perlstein, J.; Whitten, D. G. *J. Am. Chem. Soc.* **1997**, *119*, 9144.
(44) Santos Jr. D. S.; Mendonca, C. R.; Balogh, D. T.; Dhanabalan, A.; Cavalli, A.; Misoguti, L.; Giacometti, J. A.; Zilio, S. C.; Oliveira, Jr., O. N. *Chem. Phys. Lett.* **2000**, *317*, 1.
(45) Wang, X.; Balasubramanian, S.; Kumar, J.; Tripathy, S. K. *Chem. Mater.* **1998**, *10*, 1546.
(46) Anzai, J. I.; Osa, T. *Tetrahedron* **1994**, *50*, 4039.
(47) Dhanabalan, A.; Balogh, D. T.; Mendonca, C.; Riul, Jr. A.; Constantino, C. J. L.; Giacometti, J. A.; Zilio, S. C.; Oliveira, O. N., Jr. *Langmuir* **1998**, *14*, 3614.
(48) Dhanabalan, A.; Mendonca, C. R.; Balogh, D. T.; Misoguti, L.; Constantino, C. J. L.; Giacometti, J. A.; Zilio, S. C.; Oliveira, O. N., Jr. *Macromolecules* **1999**, *32*, 5277.
(49) Norris, R. K.; Sternhell, S. *Aust. J. Chem.* **1971**, *24*, 1449.
(50) Norris, R. K.; Sternhell, S. *Aust. J. Chem.* **1966**, *19*, 841.
(51) Kitano, H.; Mori, T.; Takeuchi, Y.; Tada, S.; Gemmei-Ide, M.; Yokoyama, Y.; Tanaka, M. *Macromol. Biosci.* **2005**, *5*, 314.
(52) Koetse, M.; Laschewsky, A.; Mayer, B.; Rolland, O.; Wischerhoff, E. *Macromolecules* **1998**, *31*, 9316.
(53) Decher, G.; Hong, J. D. *Makromol. Chem., Makromol. Symp.* **1991**, *46*, 321.
(54) Hong, J. D.; Decher, G.; Schmitt, J. *Thin Solid Films* **1992**, *210*, 831.
(55) Stumpe, J.; Fischer, T.; Menzel, H. *Macromolecules* **1996**, *29*, 2831.
(56) Rau, H. In *Photoisomerization of Azobenzenes in Photochemistry and Photophysics*; Rabek, J. F., Ed.; CRC Press: Boca Raton, FL, 1990; Vol. II, pp 119−141.
(57) Wu, Y.; Demachi, Y.; Tsutsumi, O.; Kanazawa, A.; Shiono, T.; Ikeda, T. *Macromolecules* **1998**, *31*, 4457.
(58) Ho, C.-H.; Yang, K.-N.; Lee, S.-N. *J. Polym. Sci., Part A: Polym. Chem.* **2001**, *39*, 2296.
(59) (a) Chen, M.; Yu, L.; Shi, Y.; Stear, W. *Macromolecules* **1991**, *24*, 5421. (b) Naito, T.; Horie, K.; Mita, I. *Polym. J.* **1991**, *23*, 809. (c) Zhang, H.-Q.; Hung, W.-Q.; Li, C.-X.; He, B.-L. *Eur. Polym. J.* **1998**, *34*, 1521. (d) Okano, K.; Shishido, A.; Iketa, T. *Macromolecules* **2006**, *39*, 145.
(60) Sin, S. L.; Gan, L. H.; Hu, X.; Tam, K. C.; Gan, Y. Y. *Macromolecules* **2005**, *38*, 3943.
(61) Mita, I.; Horie, K.; Hirao, K. *Macromolecules* **1989**, *22*, 558.
(62) Imai, Y.; Naka, K.; Chujo, Y. *Macromolecules* **1999**, *32*, 1013.

MA060169I